ANALYZING THE WEIGHTED NUCLEAR NORM MINIMIZATION AND NUCLEAR NORM MINIMIZATION BASED ON GROUP SPARSE REPRESENTATION

Zhiyuan Zha, Xinggan Zhang, Yu Wu, Qiong Wang, Yechao Bai and Lan Tang

School of Electronic Science and Engineering, Nanjing University, Nanjing 210023, China.

ABSTRACT

Nuclear norm minimization (NNM) tends to over-shrink the rank components and treats the different rank components equally, thus limits its capability and flexibility. Recent studies have shown that the weighted nuclear norm minimization (WNNM) is expected to be more accurate than NNM. However, it still lacks a plausible mathematical explanation why WNNM is more accurate than NNM. This paper analyzes the WNNM and NNM from the perspective of the group sparse representation (GSR). In particular, an adaptive dictionary for each group is designed to connect the rank minimization and GSR models. Then, we prove that the rank minimization model is equivalent to GSR model. Based on that conclusion, we show mathematically that WNNM is more accurate than NNM. To make the proposed model tractable and robust, the alternative direction multiplier method (ADMM) framework is developed to solve the proposed model. Experimental results on two low-level vison applications, image deblurring and image compressive sensing (CS) recovery, demonstrate that the proposed scheme outperforms many state-of-the-art methods both quantitatively and qualitatively.

Index Terms— Low rank, WNNM, NNM, GSR, rank minimization, ADMM.

1. INTRODUCTION

Since the data from many practical cases have low rank property in essence, low rank matrix approximation (LRMA), which aims to recover the underlying low rank structure from its degraded/corrupted samples, has a wide range of applications in machine learning and computer vision [1, 2, 3]. For instance, the Netflix customer data matrix is regarded as low rank because the customers' choices are mostly affected by a few common factors [1]. As the matrix formed by nonlocal similar patches in a natural image is of low rank, a flurry of matrix completion problems have been proposed, such as collaborative filtering [2], reconstruction of occluded/corrupted face images [3], etc.

Generally speaking, methods dealing with LRMA can be classified into two categories: the low rank matrix factorization

Email: zhazhiyuan.mmd@gmail.com.

(LRMF) methods [4, 5] and the nuclear norm (rank) minimization (NNM) methods [2, 6, 7]. In this work we focus on the latter category. The nuclear norm of a matrix X denoted by $||X||_*$, is the sum of its singular values, i.e., $||X||_* = \sum_i \sigma_i(X)$, where $\sigma_i(X)$ is the i-th singular value of the matrix X. NNM aims to recover the underlying low rank matrix X from its degraded observation matrix Y, by minimizing $||X||_*$. In recent years, a flurry of NNM-based methods have been developed, such as robust principle component analyze (RPCA) [7], and low rank representation for subspace segmentation [8].

Although NNM has been widely used for low rank matrix approximation, it often ignores the prior knowledge about the singular values of a practical data matrix among which larger ones measure the underlying principle components information. For example, the large singular values of a matrix of image similar patches characterize the major edge and texture information. This means that to recover an image from its degraded/corrupted one, we should shrink larger singular values less and smaller ones more. In a nutshell, NNM is not flexible enough since it treats singular values equally and tends to over-shrink the singular values.

To improve the flexibility of NNM, the weighted nuclear norm minimization (WNNM) model is proposed [9, 10, 32, 33]. The weighted nuclear norm of a data matrix X is defined as $||X||_{\mathbf{w},*} = \sum_i w_i \sigma_i(X)$, where $\mathbf{w} = [w_1, w_2, ..., w_i]$ and $w_i > 0$ is a non-negative weight assigned to $\sigma_i(X)$. Recent works have demonstrated that WNNM can obtain more accurate results than NNM in various machine learning and computer vision applications [11, 12]. However, mathematically, we are still not clear why WNNM is more accurate than NNM.

With the above consideration, we analyze the WNNM and NNM from the group sparse representation (GSR) perspective. To the best of our knowledge, few works analyze why WNNM is more accurate than NNM mathematically. The contribution of this paper is as follows. First, an adaptive dictionary for each group is designed to connect the rank minimization and GSR models. Second, we prove that the equivalence of rank minimization and GSR models. Based on that conclusion, we show mathematically that WNNM is more accurate than NNM. Third, to make the optimization tractable, we adopt the alternating direction method of multipliers (ADMM) to solve the proposed model. Experimental results on two low-level vision

applications, image deblurring and image compressive sensing (CS) recovery, show that the proposed scheme outperforms many state-of-the-art methods.

2. RELATED WORK

2.1. Group Sparse Representation

Traditional patch-based sparse representation model [13] usually suffers from some limits, such as dictionary learning with great computational complexity and neglecting the correlations between sparsely-coded patches [14, 15].

Instead of using patch as the basic unit of sparse representation, group sparse representation (GSR) presents a powerful mechanism, which combines local sparsity and nonlocal selfsimilarity of images simultaneously in a unified framework [15]. Specifically, an image X with size N is divided into n overlapped patches of size $\sqrt{m} \times \sqrt{m}$, and each patch is denoted by the vector $\mathbf{x}_i \in \mathbb{R}^m, i = 1, 2, ..., n$. Then for each exemplar patch x_i , its k similar patches are selected from a $R \times R$ sized search window to form a set S_i . Since then, all the patches in S_i are stacked into a data matrix of size $m \times k$, denoted by X_i , which includes every patch in X_i as its columns, i.e., $X_i = \{x_{i,1}, x_{i,2}, ..., x_{i,k}\}$. The matrix X_i consisting of all the patches with similar structures is called as a group, where $x_{i,k}$ denotes the k-th similar patch of the i-th group. Finally, similar to patch-based sparse representation [13], given a dictionary D_i , each group X_i can be sparsely represented as $\alpha_i = \boldsymbol{D}_i^{-1} \boldsymbol{X}_i$ and solved by the following ℓ_0 -norm minimization problem,

$$\alpha_i = \arg\min_{\alpha_i} \frac{1}{2} || \boldsymbol{X}_i - \boldsymbol{D}_i \boldsymbol{\alpha}_i ||_F^2 + \lambda_i || \boldsymbol{\alpha}_i ||_0$$
 (1)

where $|| \bullet ||_F^2$ denotes the Frobenius norm and λ_i is the regularization parameter. $|| \bullet ||_0$ is ℓ_0 norm, counting the nonzero entries of α_i .

However, since the ℓ_0 minimization is discontinuous optimization and NP-hard, Eq. (1) is a difficult combinatorial optimization problem. For this reason, it has been suggested that the non-convex ℓ_0 minimization can be replaced by its convex ℓ_1 counterpart,

$$\alpha_i = \arg\min_{\alpha_i} \frac{1}{2} ||X_i - D_i \alpha_i||_F^2 + \lambda_i ||\alpha_i||_1$$
 (2)

Nonetheless, a fact that cannot be ignored is that ℓ_1 minimization is hard to achieve the desired sparsity solution in some practical problems, such as image inverse problems [16].

2.2. Reweighted ℓ_1 Norm Minimization

To improve the sparsity of ℓ_1 norm, Candès *et al.* [17] proposed the weighted ℓ_1 norm to replace the ℓ_1 norm,

$$\alpha_i = \arg\min_{\alpha_i} \frac{1}{2} ||X_i - D_i \alpha_i||_F^2 + \lambda_i ||\mathbf{w}_i \alpha_i||_1$$
 (3)

where w_i is the positive weights. Note that, different from ℓ_0 minimization problem in Eq. (1) is non-convex, solving Eq. (3) is a convex optimization problem. Also, the proposition is given as follows,

Proposition 1 ([17]).

$$||\mathbf{w}_i \alpha_i||_1 \succ ||\alpha_i||_1 \tag{4}$$

where $v_1 \succ v_2$ denotes that the entry v_1 has much more sparsity encouraging than the entry v_2 .

3. WHY WNNM IS MORE ACCURATE THAN NNM

As far as we know, the weighted nuclear norm minimization (WNNM) can achieve more accurate results than nuclear norm minimization (NNM). However, so far, we are still not clear why WNNM is more accurate than NNM because it lacks a feasible mathematical derivation. In this section, we analyze the WNNM and NNM from the group sparse representation (GSR) perspective. First, we introduce the related works of NNM and WNNM. Second, an adaptive dictionary for each group is designed to connect the rank minimization and GSR models. Third, we prove that the equivalence of the rank minimization and GSR models, and thus, we further show mathematically that WNNM is more accurate than NNM.

3.1. Nuclear Norm Minimization

According to [6], nuclear norm is the tightest convex relaxation of the original rank minimization problem. Given a data matrix $Y \in \Re^{m \times k}$, the goal of NNM is to find a matrix $X \in \Re^{m \times k}$ of rank r, which satisfies the following objective function,

$$\hat{X} = \arg\min_{X} \frac{1}{2} ||Y - X||_F^2 + \lambda ||X||_*$$
 (5)

where $||X||_* = \sum_i \sigma_i(X)$, and $\sigma_i(X)$ is the *i*-th singular value of the matrix X. λ is a positive constant. Candès *et al*. [18] showed that the low rank matrix can be perfectly recovered from the degraded/corrupted data matrix with high probability by solving an NNM problem. Cai *et al*. [2] proved that NNM problem can be easily solved by imposing a soft-thresholding operation, that is, the solution of Eq. (5) which can be solved by

$$\hat{\mathbf{X}} = \mathbf{U}\mathbf{S}_{\lambda}(\mathbf{\Sigma})\mathbf{V}^{T} \tag{6}$$

where $Y = U\Sigma V^T$ is the SVD of Y and $S_{\lambda}(\Sigma)$ is the soft-thresholding operator function on diagonal matrix Σ with parameter λ . For each diagonal element Σ_{ii} in Σ , there is $S_{\lambda}(\Sigma)_{ii} = \operatorname{soft}(\Sigma_{ii}, \lambda) = \max(\Sigma_{ii} - \lambda, 0)$.

More Specifically, they proved the following theorem.

Theorem 1 ([2]). For each $\lambda \geq 0$ and Y, the singular value shrinkage operator Eq. (6) obeys Eq. (5).

3.2. Weighted Nuclear Norm Minimization

As an alternative, the weighted nuclear norm minimization (WNNM) model is proposed [9, 10, 32, 33]. That is, the weighted nuclear norm $||X||_{w,*}$ used to regularize X and Eq. (5) can be rewritten as

$$\hat{X} = \arg\min_{X} \frac{1}{2} ||Y - X||_{F}^{2} + ||X||_{w,*}$$
 (7)

where $||X||_{\mathbf{w},*} = \sum_i w_i \sigma_i(X)$, $\mathbf{w} = [w_1, w_2, ..., w_i]$ and $w_i > 0$ is a non-negative weight assigned to $\sigma_i(X)$. Also, Gu *et al.* [9] proved the following theorem.

Theorem 2 ([9]). If the singular values $\sigma_1 \ge ... \ge \sigma_{n_0}$ and the weights satisfy $0 \le w_1 \le ... w_{n_0}$, $n_0 = \min(m, k)$, the WNNM problem in Eq. (7) has a globally optimal solution

$$\hat{X} = US_w(\Sigma)V^T \tag{8}$$

where $Y = U\Sigma V^T$ is the SVD of Y and $S_w(\Sigma)$ is the generalized soft-thresholding operator with the weighted vector w, i.e., $S_w(\Sigma)_{ii} = \text{soft}(\Sigma_{ii}, w_i) = \max(\Sigma_{ii} - w_i, 0)$.

To prove that WNNM is more accurate than NNM, we have the following theorem.

Theorem 3. For $0 \le w_1 \le ...w_{n_0}$ and Y, $n_0 = \min(m, k)$, the singular value shrinkage operator Eq. (8) satisfies Eq. (7). *Proof:* see Appendix.

Note that the relationship between Theorem 3 is the necessary and sufficient condition of Theorem 2.

3.3. Adaptive Dictionary Learning

In this subsection, an adaptive dictionary learning approach is designed. To be concrete, for each group X_i , its adaptive dictionary can be learned from its observation $Y_i \in \Re^{m \times k}$.

Then, we apply the singular value decomposition (SVD) to Y_i ,

$$Y_i = U_i \Sigma_i V_i^T = \sum_{j=1}^{n_0} \sigma_{i,j} u_{i,j} v_{i,j}^T$$
 (9)

where $\mu_i = [\sigma_{i,1}, \sigma_{i,2}, ..., \sigma_{i,n_0}], n_0 = \min(m, k), \Sigma_i = \operatorname{diag}(\mu_i)$ is a diagonal matrix whose non-zero elements are represented by μ_i , and $u_{i,j}, v_{i,j}$ are the columns of U_i and V_i , respectively.

Moreover, we define each dictionary atom $d_{i,j}$ of the adaptive dictionary D_i for each group Y_i as follows:

$$\boldsymbol{d}_{i,j} = \boldsymbol{u}_{i,j} \boldsymbol{v}_{i,j}^T, \quad j = 1, 2, ..., n_0$$
 (10)

Finally, learning an adaptive dictionary from each group Y_i can be constructed by $D_i = [d_{i,1}, d_{i,2}, ..., d_{i,n_0}]$. The proposed dictionary learning approach is efficient due to the fact that it only requires one SVD operator for each group.

3.4. WNNM is More Accurate than NNM

To prove that WNNM is more accurate than NNM, we need the following lemmas:

Lemma 1 ([19]). The minimization problem

$$x = \arg\min_{x} \frac{1}{2} ||x - a||_{2}^{2} + \tau \cdot ||x||_{1}$$
 (11)

has a closed-form solution, which can be expressed as

$$\hat{\mathbf{x}} = \operatorname{soft}(\mathbf{a}, \tau) = \operatorname{sgn}(\mathbf{a}, \tau) \cdot \max(abs(\mathbf{a}) - \tau, 0)$$
 (12)

Lemma 2. For the following optimization problem

$$\min_{x_i \ge 0} \frac{1}{2} \sum_{i=1}^{n} (x_i - a_i)^2 + w_i x_i \tag{13}$$

If $a_1 \ge ... \ge a_n \ge 0$ and the weights satisfy $0 \le w_1 \le ... w_n$, then the global optimum of Eq. (13) is $\hat{x}_i = \operatorname{soft}(a_i, w_i) = \max(a_i - w_i, 0)$.

Proof: see Appendix.

Now, the ℓ_1 norm-based group sparse representation problem can be expressed in Eq. (2). According to the above design of adaptive dictionary D_i in Eq. (10), we have the following theorem.

Theorem 4.

$$||Y_i - X_i||_F^2 = ||\mu_i - \alpha_i||_2^2$$
 (14)

where $Y_i = D_i \mu_i$ and $X_i = D_i \alpha_i$.

Proof: see Appendix.

Therefore, based on Proposition 1, Lemma (1, 2) and Theorem (1, 2, 3, 4), we can prove that

Proposition 2. WNNM is more accurate than NNM under the adaptive dictionary D_i .

Proof: see Appendix.

Note that the main difference between sparse representation model and the rank minimization model is that sparse representation model has a dictionary learning operator and the rank minimization model does not involve.

4. IMAGE RESTORATION USING GROUP SPARSE REPRESENTATION VIA THE WEIGHTED ℓ_1 MINIMIZATION

In this section, we demonstrate the proposed scheme in the application of image restoration (IR), including image debluring and image compressive sensing (CS) recovery. The goal of IR tasks is to reconstruct a high quality image \boldsymbol{X} from its degraded observation \boldsymbol{Y} , which is a typical ill-posed inverse problem and can be mathematically expressed as

$$Y = HX + \varphi \tag{15}$$

where X, Y denote the original image and the degraded image, respectively. H is the degraded operator and φ is usually assumed to be additive white Gaussian noise.

In the scenario of IR, what we observed is the degraded image Y in Eq. (15), and thus we utilize GSR model to reconstruct

X from **Y** by solving the following weighted ℓ_1 minimization problem,

$$\alpha = \arg\min_{\alpha} \frac{1}{2} ||\mathbf{Y} - \mathbf{H} \mathbf{D} \alpha||_{2}^{2} + \lambda ||\mathbf{w} \alpha||_{1}$$
 (16)

where λ is a regularization parameter.

The problem in Eq. (16) can be solved by the iterative shrinkage (IST) algorithm [20]. However, the major drawback of the IST algorithm is its low convergence speed. In this paper, we adopt the algorithm framework of the alternating direction method of multipliers (ADMM) [21] to solve Eq. (16). Specifically, we introduce an auxiliary variable U and Eq. (16) can be rewritten as

$$\alpha = \arg\min_{U,\alpha} \frac{1}{2} ||Y - HU||_2^2 + \lambda ||w\alpha||_1, \quad s.t. \quad U = D\alpha \quad (17)$$

Therefore, Eq. (17) can be turned into three iterative steps:

$$U^{t+1} = \arg\min_{U} \frac{1}{2} ||Y - HU||_{2}^{2} + \frac{\rho}{2} ||U - D\alpha^{t} - C^{t}||_{2}^{2}$$
(18)

$$\boldsymbol{\alpha}^{t+1} = \arg\min_{\boldsymbol{\alpha}} \lambda ||\boldsymbol{w}\boldsymbol{\alpha}||_1 + \frac{\rho}{2}||\boldsymbol{U}^{t+1} - \boldsymbol{D}\boldsymbol{\alpha} - \boldsymbol{C}^t||_2^2 \quad (19)$$

$$C^{t+1} = C^t - (U^{t+1} - D\alpha^{t+1})$$
 (20)

Obviously, One can observe that the minimization for Eq. (17) can be separated into two minimization sub-problems, i.e., U and α sub-problems. We will show that there is an efficient solution to each sub-problem. To avoid confusion, the subscribe t may be omitted for conciseness.

U Sub-problem

Given α , the U sub-problem denoted by Eq. (18) becomes

$$\min_{U} Q_1(U) = \min_{U} \frac{1}{2} ||Y - HU||_2^2 + \frac{\rho}{2} ||U - D\alpha - C||_2^2$$
(21)

Clearly, Eq. (21) has a closed-form solution and its solution can be expressed as

$$\hat{\boldsymbol{U}} = (\boldsymbol{H}^T \boldsymbol{H} + \rho \boldsymbol{I})^{-1} (\boldsymbol{H}^T \boldsymbol{Y} + \rho (\boldsymbol{D} \boldsymbol{\alpha} + \boldsymbol{C}))$$
 (22)

where I represents the identity matrix.

α Sub-problem

Given U, similarly, according to Eq. (19), the α subproblem can be written as

$$\min_{\alpha} \mathbf{Q}_{2}(\alpha) = \min_{\alpha} \frac{1}{2} ||\mathbf{D}\alpha - \mathbf{L}||_{2}^{2} + \frac{\lambda}{\rho} ||\mathbf{w}\alpha||_{1}$$
 (23)

where L = U - C. However, due to the complex definition of $||w\alpha||_1$, it is difficult to solve Eq. (23) directly. Let $X = D\alpha$, Eq. (23) can be rewritten as

$$\min_{\alpha} \mathbf{Q}_2(\alpha) = \min_{\alpha} \frac{1}{2} ||\mathbf{X} - \mathbf{L}||_2^2 + \frac{\lambda}{\rho} ||\mathbf{w}\alpha||_1$$
 (24)

To make Eq. (24) tractable, a general assumption is made, with which even a closed-form solution of Eq. (24) can be achieved. More specifically, L can be regarded as some type of noisy observation of X, and thus R = X - L follows an independent zero mean distribution with variances δ^2 . The following theorem can be proven with this assumption.

Theorem 5. Defining $X, L \in \mathbb{R}^N$, $X_i, L_i \in \mathbb{R}^{m \times k}$, and e(j)as each element of error vector e, where e = X - L, i =1, ..., N. Assume that e(j) follows an independent zero mean distribution with variance δ^2 , and thus for any $\varepsilon > 0$, we can represent the relationship between $\frac{1}{N}||X-L||_2^2$ and $\frac{1}{K}\sum_{i=1}^{n}||X_i-L_i||_2^2$ by the following property,

$$\lim_{\substack{N \to \infty \\ K \to \infty}} P\{|\frac{1}{N}||X - L||_2^2 - \frac{1}{K} \sum_{i=1}^n ||X_i - L_i||_F^2| < \varepsilon\} = 1$$
(25)

where $P(\bullet)$ represents the probability and $K = m \times k \times n$. *Proof:* see Appendix.

Thus, based on *Theorem 5*, we have the following equation with a very large probability (restricted 1) at each iteration,

$$\frac{1}{N}||X - L||_2^2 = \frac{1}{K} \sum_{i=1}^n ||X_i - L_i||_F^2$$
 (26)

Algorithm 1: ADMM method for for the proposed model.

Input: the observed image Y and the measurement matrix H.

Initialization: C, U, α , R, m, k, ρ , δ , ϵ , ϱ , t;

Update U^{t+1} by Eq. (22); $L^{t+1} = U^{t+1} - C^t$;

For Each group L_i :

Construct dictionary D_i by computing Eq. (10);

Update λ_i^{t+1} by computing $\lambda_i = 2\sqrt{2}\sigma^2/(\eta_i + \varrho)$;

Update τ_i^{t+1} computing by $\tau_i = \lambda_i K/\rho N$; Update w_i^{t+1} computing by $w_i = 1/(|\gamma_i| + \epsilon)$;

Update α_i^{t+1} computing by Eq. (29);

End For

Update D^{t+1} by concatenating all D_i ;

Update α^{t+1} by concatenating all α_i ;

Update C^{t+1} by computing Eq. (20);

 $t \leftarrow t + 1;$

Until

maximum iteration number is reached.

Output:

The final restored image $\hat{X} = D\hat{\alpha}$.

And thus, Eq. (24) can be rewritten as

$$\min_{\alpha} \frac{1}{2} ||X - L||_{2}^{2} + \frac{\lambda}{\rho} ||w\alpha||_{1}$$

$$= \min_{\alpha_{i}} \left(\sum_{i=1}^{n} \frac{1}{2} ||X_{i} - L_{i}||_{F}^{2} + \tau_{i} ||w_{i}\alpha_{i}||_{1} \right)$$

$$= \min_{\alpha} \left(\sum_{i=1}^{n} \frac{1}{2} ||L_{i} - D_{i}\alpha_{i}||_{F}^{2} + \tau_{i} ||w_{i}\alpha_{i}||_{1} \right)$$
(27)

where $\tau_i = \lambda_i K/\rho N$ and D_i is a dictionary. It can be seen that Eq. (27) can be regarded as a group sparse representation problem by solving n sub-problems for all the group X_i . Based on *Theorem 4*, Eq. (27) can be rewritten as

$$\hat{\alpha}_{i} = \min_{\alpha_{i}} \sum_{i=1}^{n} \frac{1}{2} ||\gamma_{i} - \alpha_{i}||_{2}^{2} + \tau_{i}||w_{i}\alpha_{i}||_{1}$$
 (28)

where $L_i = D_i \gamma_i$ and $X_i = D_i \alpha_i$. Therefore, based on *Lemma 2*, a closed-form solution of Eq. (28) can be computed as

$$\hat{\boldsymbol{\alpha}}_i = \operatorname{soft}(\boldsymbol{\gamma}_i, \tau_i w_i) = \max(abs(\boldsymbol{\gamma}_i) - \tau_i w_i, 0)$$
 (29)

For each weight w_i , large values of sparse coefficient α_i usually transmit major edge and texture information. This implies that to reconstruct X_i from its degraded one, we should shrink large values less, while shrinking smaller ones more, and thus we have $w_i = 1/(|\gamma_i| + \epsilon)$, where ϵ is a small constant. Inspired by [22], the regularization parameter λ_i of each group L_i is set as: $\lambda_i = 2\sqrt{2}\delta^2/(\eta_i + \varrho)$, where η_i denotes the estimated variance of γ_i , and ϱ is a small constant. After solving the two sub-problems, we summarize the overall algorithm for Eq. (16) in **Algorithm 1**.

5. EXPERIMENTAL RESULTS

In this section, we report our experimental results in the applications of image deblurring and image CS recovery. All the experimental images are shown in Fig. 1. Since the group sparse representation (GSR) is exploited to prove that WNNM is more accurate than NNM, we called the proposed scheme as GSR-WNNM. To verify the effectiveness of WNNM, we have implemented a variant of the GSR that use NNM, denoted as GSR-NNM.

Table 1. Average PSNR results (dB) of image Deblurring

Method	Uniform	Uniform Gaussian	
IDD-BM3D [23]	24.94	25.13	25.32
NCSR [24]	24.96	25.15	25.19
FPD [25]	24.02	25.02	24.46
MSEPLL [26]	24.14	24.98	24.78
GSR-NNM	24.15	24.49	24.46
GSR-WNNM	25.35	25.39	25.80

In image deblurring, we have compared the GSR-WNNM with five other competing approaches: IDD-BM3D [23], NCSR [24], FPD [25], MSEPLL [26] and GSR-NNM. In our comparative study, three blur kernels, 9×9 uniform kernel, a Gaussian kernel (fspecial('gaussian', 25, 1.6)) and a motion kernel (fspecial('motion', 20, 45)) are used. Blurred images are further corrupted by additive white Gaussian noise with $\delta=2$. The searching window $R\times R$ is set to be 40×40 and searching matched patches k=60. The size of each patch $\sqrt{m}\times \sqrt{m}$ is set to be 8×8 . We assign $\varrho=0.1$ and $\epsilon=0.35$. $\varrho=0.0225$, 0.0225 and 0.0375 for uniform, Gaussian and motion kernel, respectively.

Table 1 lists the average PSNR comparison results for a collection of 8 color images among six competing methods. It can be seen that GSR-WNNM outperforms other methods for all three types of blur kernels. The visual comparison of the deblurring methods is shown in Fig. 2. It can be seen that the NCSR, FPD, MSEPLL and GSR-NNM still generate some undesirable artifacts, while IDD-BM3D results in over-smooth phenomena. By contrast, the GSR-WNNM is able to preserve the sharpness of edges and suppress undesirable artifacts more effectively than other competing methods.

Table 2. Average PSNR results (dB) of image CS recovery

Method	0.1	0.2	0.3	0.4
BCS [27]	23.97	26.57	28.52	30.27
BM3D-CS [28]	24.70	30.69	34.16	37.14
ADS-CS [29]	27.82	32.43	35.53	37.99
SGSR [30]	27.91	32.20	34.84	36.92
MRK [31]	27.62	31.63	34.78	37.18
GSR-NNM	27.07	30.59	32.27	33.52
GSR-WNNM	29.37	33.73	36.65	38.95

In image CS recovery, we generate the CS measurements at the block level by utilizing a Gaussian random projection matrix to test images, i.e, the block-based CS recovery with block size of 32×32 . The searching window $R \times R$ is set to be 20×20 and searching matched patches k = 60. $\rho = 0.03$ for 0.1N measurements, and $\rho = 0.1$ for other measurements. ϱ and $\epsilon = 0.35$. The size of each patch $\sqrt{m} \times \sqrt{m}$ is set to be 6×6 . To verify the performance of the GSR-WNNM, we have compared it with some competitive CS recovery methods including the BCS [27], BM3D-CS [28], ADS-CS [29], SGSR [30], MRK [31] and GSR-NNM.

The average PSNR results of gray images are shown in Table 2. It can be seen that GSR-WNNM outperforms other methods over different numbers of CS measurements. The average gain of GSR-WNNM over BCS, BM3D-CS, ADS-CS, SGSR, MRK and GSR-NNM can be as much as 7.34dB, 3.00dB, 1.23dB, 1.71dB, 1.87dB and 3.81dB, respectively. The visual comparison of the image CS recovery is shown Fig. 3. It can be seen that BCS generates the worst perceptual result. The BM3D-CS, ADS-CS, SGSR, MRK, and GSR-NNM methods can obtain much better visual quality than BCS method, but still suffer from some undesirable artifacts or over-smooth phenomena, such as ring effects and loss of some fine image details. In contrast, GSR-WNNM not only removes most of the visual artifacts, but also preserves large-scale sharp edges and small-scale fine image details more effectively in comparison with other competing methods.

According to the above analysis, it can be seen that GSR-WNNM significantly outperforms GSR-NNM. Therefore, the above analysis are indirect evidence that WNNM is more accurate than NNM.



Fig. 1. All test images.



Fig. 2. Visual comparison of *Barbara* by image deblurring with Gaussian blur: fspecial ('gaussian', 25, 1.6), $\delta = 2$.

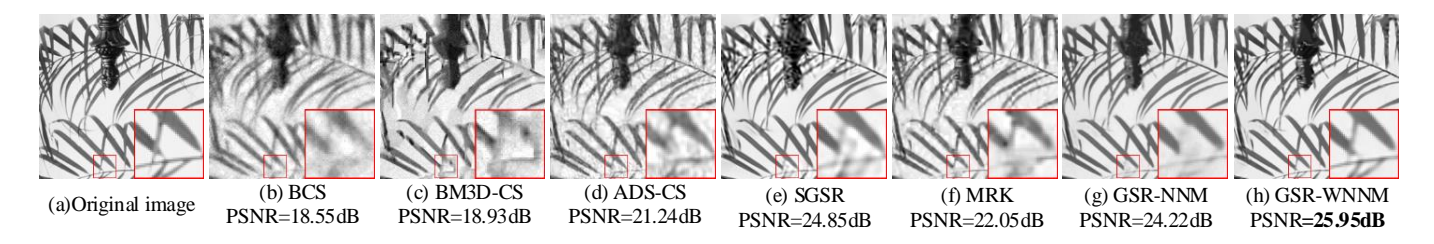


Fig. 3. Visual comparison of *Leaves* by CS recovery with 0.1 N measurements.

6. CONCLUSION

This paper analyzed the weighted nuclear norm minimization(WNNM) and nuclear norm minimization (NNM) based on group sparse representation (GSR). We designed an adaptive dictionary for each group to connect the rank minimization and GSR models. We proved that the equivalence of the rank minimization and GSR models. Based on that conclusion, we showed mathematically that WNNM is more accurate than NNM. To make the proposed model tractable and robust, the alternative direction multiplier method (ADMM) framework was adopted to solve the proposed model. Experimental results on two low-level vision applications, i.e., image deblurring and image CS recovery, have demonstrated that the proposed scheme outperforms many state-of-the-art methods both quantitatively and qualitatively.

7. APPENDIX

Theorem 3. For $0 \le w_1 \le ...w_{n_0}$ and Y, $n_0 = \min(m, k)$, the singular value shrinkage operator Eq. (8) satisfies Eq. (7).

Proof. For fixed weights W, $h_0(X) = \frac{1}{2}||Y - X||_F^2 + ||X||_{w,*}$, \hat{X} minimizes h_0 if and only if it satisfies the following optimal condition,

$$\mathbf{0} \in \hat{\mathbf{X}} - \mathbf{Y} + \partial ||\hat{\mathbf{X}}||_{\mathbf{w},*} \tag{30}$$

where $\partial ||\hat{X}||_{w,*}$ is the set of subgradients of the weighted nuclear norm. Let matrix $X \in \Re^{m \times k}$ be an arbitrary matrix

and its SVD be $U\Sigma V^T$. It is known from [18, 34] that the subgradient of $||X||_{w,*}$ can be derived as

$$\partial ||\mathbf{X}||_{\mathbf{w},*} = \{\mathbf{U}\mathbf{W}_r\mathbf{V}^T + \mathbf{Z} : \mathbf{Z} \in \Re^{m \times k}, \mathbf{U}^T\mathbf{Z} = \mathbf{0}, \\ \mathbf{Z}\mathbf{V} = \mathbf{0}, \sigma_j(\mathbf{Z}) \le w_{r+j}, j = 1, ..., n_0 - r\}$$
(31)

where r is the rank of X and W_r is the diagonal matrix composed of the first r rows and r columns of the diagonal matrix diag (W). Note that the sub-gradient conclusion in Eqs. (30) and (31) has been proved for convex problem [2]. Nonetheless, they are feasible for non-convex problem [35].

In order to show that \hat{X} obeys Eq. (31), the SVD of Y can be rewritten as

$$Y = U_0 \Sigma_0 V_0^T + U_1 \Sigma_1 V_1^T \tag{32}$$

where U_0 , V_0 (resp. U_1 , V_1) are the singular vectors associated with singular values greater than w_j (resp. smaller than or equal to w_j). With these notations, we have

$$\hat{\mathbf{X}} = \mathbf{U}_0(\mathbf{\Sigma}_0 - \mathbf{W}_r)\mathbf{V}_0^T \tag{33}$$

Therefore,

$$\boldsymbol{Y} - \hat{\boldsymbol{X}} = \boldsymbol{U}_0 \boldsymbol{W}_r \boldsymbol{V}_0^T + \boldsymbol{Z} \tag{34}$$

where $\mathbf{Z} = \mathbf{U}_1 \mathbf{\Sigma}_1 \mathbf{V}_1^T$, by definition, $\mathbf{U}_0^T \mathbf{Z} = \mathbf{0}, \mathbf{Z} \mathbf{V}_0 = \mathbf{0}$ and since the diagonal elements of $\mathbf{\Sigma}_1$ are smaller than w_{j+r} , it is easy to verify that $\boldsymbol{\sigma}_j \leq w_{r+j}, j=1,2,...,n_0-r$. Thus, $\mathbf{Y} - \hat{\mathbf{X}} \in \partial ||\hat{\mathbf{X}}||_{\mathbf{w},*}$, which concludes the proof.

Lemma 2. For the following optimization problem

$$\min_{x_i \ge 0} \frac{1}{2} \sum_{i=1}^{n} (x_i - a_i)^2 + w_i x_i \tag{35}$$

If $a_1 \ge ... \ge a_n \ge 0$ and the weights satisfy $0 \le w_1 \le ... w_n$, then the global optimum of Eq. (35) is $\hat{x}_i = \operatorname{soft}(a_i, w_i) = \max(a_i - w_i, 0)$.

Proof. Without considering the constraint, the optimization problem Eq. (35) can be rewritten as the following unconstrained form,

$$\min_{x_i \ge 0} \frac{1}{2} (x_i - a_i)^2 + w_i x_i \Leftrightarrow \min_{x_i \ge 0} \frac{1}{2} (x_i - (a_i - w_i))^2$$
 (36)

Thus, it can be easily derived that the global optimization solution of Eq. (36) is

$$\hat{x}_i = \max(a_i - w_i, 0), i = 1, 2, ...n.$$
(37)

As we have $a_1 \ge ... \ge a_n \ge 0$ and the weights $0 \le w_1 \le ... w_n$, it can be seen that $\hat{x}_1 \ge \hat{x}_2 \ge ... \ge \hat{x}_n$. Thus, $\hat{x}_{i=1,2,...,n}$ obeys the constraint of Eq. (35), and thus $\hat{x}_i = \max(a_i - w_i, 0)$ is the global solution of Eq. (35).

Theorem 4.

$$||Y_i - X_i||_F^2 = ||\mu_i - \alpha_i||_2^2$$
 (38)

where $Y_i = D_i \mu_i$ and $X_i = D_i \alpha_i$.

Proof. Since the adaptive dictionary D_i is constructed by Eq. (10), and the unitary property of U_i and V_i , we have

$$||Y_{i} - X_{i}||_{F}^{2} = ||D_{i}(\mu_{i} - \alpha_{i})||_{F}^{2} = ||U_{i}\operatorname{diag}(\mu_{i} - \alpha_{i})V_{i}||_{F}^{2}$$

$$= \operatorname{trace}(U_{i}\operatorname{diag}(\mu_{i} - \alpha_{i})V_{i}V_{i}^{T}\operatorname{diag}(\mu_{i} - \alpha_{i})U_{i}^{T})$$

$$= \operatorname{trace}(U_{i}\operatorname{diag}(\mu_{i} - \alpha_{i})\operatorname{diag}(\mu_{i} - \alpha_{i})U_{i}^{T})$$

$$= \operatorname{trace}(\operatorname{diag}(\mu_{i} - \alpha_{i})U_{i}U_{i}^{T}\operatorname{diag}(\mu_{i} - \alpha_{i}))$$

$$= \operatorname{trace}(\operatorname{diag}(\mu_{i} - \alpha_{i})\operatorname{diag}(\mu_{i} - \alpha_{i}))$$

$$= ||\mu_{i} - \alpha_{i}||_{2}^{2}$$
(39)

Proposition 2. WNNM is more accurate than NNM under the adaptive dictionary D_i .

Proof. On the basis of *Theorem 4*, we have

$$\boldsymbol{\alpha}_{i} = \arg\min_{\boldsymbol{\alpha}_{i}} \frac{1}{2} ||\boldsymbol{Y}_{i} - \boldsymbol{D}_{i} \boldsymbol{\alpha}_{i}||_{F}^{2} + \lambda_{i} ||\boldsymbol{\alpha}_{i}||_{1}$$

$$= \arg\min_{\boldsymbol{\alpha}_{i}} \frac{1}{2} ||\boldsymbol{\mu}_{i} - \boldsymbol{\alpha}_{i}||_{2}^{2} + \lambda_{i} ||\boldsymbol{\alpha}_{i}||_{1}$$
(40)

Thus, based on Lemma 1, we have

$$\alpha_i = \operatorname{soft}(\mu_i, \lambda_i) = \max(abs(\mu_i) - \lambda_i, 0)$$
 (41)

Obviously, according to Eqs. (9) and (10), we have

$$\hat{\boldsymbol{X}}_{i} = \boldsymbol{D}_{i} \boldsymbol{\alpha}_{i} = \sum_{j=1}^{n_{0}} \operatorname{soft}(\boldsymbol{\mu}_{i,j}, \lambda_{i}) \boldsymbol{d}_{i,j}$$

$$= \sum_{j=1}^{n_{0}} \operatorname{soft}(\boldsymbol{\mu}_{i,j}, \lambda_{i}) \boldsymbol{u}_{i,j} \boldsymbol{v}_{i,j}^{T}$$

$$= \boldsymbol{U}_{i} \boldsymbol{S}_{\lambda_{i}}(\boldsymbol{\Sigma}_{i}) \boldsymbol{V}_{i}^{T}$$
(42)

where $\mu_{i,j}$ represents the *j*-th element of the *i*-th group sparse coefficient μ_i , and Σ_i is the singular value matrix of the *i*-th group Y_i .

Thus, based on *Theorem 1*, we prove that the ℓ_1 -norm based GSR problem (Eq. (40)) is equivalent to the NNM problem (Eq. (5)).

Similarly, based on *Theorem 4*, for the weighted ℓ_1 normbased group sparse representation problem, we have

$$\boldsymbol{\alpha}_{i} = \arg\min_{\boldsymbol{\alpha}_{i}} \frac{1}{2} ||\boldsymbol{Y}_{i} - \boldsymbol{D}_{i} \boldsymbol{\alpha}_{i}||_{F}^{2} + ||\boldsymbol{w}_{i} \boldsymbol{\alpha}_{i}||_{1}$$

$$= \arg\min_{\boldsymbol{\alpha}_{i}} \frac{1}{2} ||\boldsymbol{\mu}_{i} - \boldsymbol{\alpha}_{i}||_{2}^{2} + ||\boldsymbol{w}_{i} \boldsymbol{\alpha}_{i}||_{1}$$
(43)

Thus, based on Lemma 2, we have

$$\alpha_i = \operatorname{soft}(\boldsymbol{\mu}_i, \boldsymbol{w}_i) = \max(\boldsymbol{\mu}_i - \boldsymbol{w}_i, 0) \tag{44}$$

Based on Eqs. (9) and (10), we have

$$\hat{X}_{i} = \mathbf{D}_{i} \boldsymbol{\alpha}_{i} = \sum_{j=1}^{n_{0}} \operatorname{soft}(\boldsymbol{\mu}_{i,j}, \boldsymbol{w}_{i}) \boldsymbol{d}_{i,j}
= \sum_{j=1}^{n_{0}} \operatorname{soft}(\boldsymbol{\mu}_{i,j}, \boldsymbol{w}_{i}) \boldsymbol{u}_{i,j} \boldsymbol{v}_{i,j}^{T}
= \boldsymbol{U}_{i} \mathbf{S}_{\boldsymbol{w}_{i}}(\boldsymbol{\Sigma}_{i}) \boldsymbol{V}_{i}^{T}$$
(45)

Therefore, based on *Theorem 3*, we prove that the weighted ℓ_1 norm-based GSR problem (Eq. (43)) is equivalent to the WNNM problem (Eq. (7)).

Proposition 1 has showed that the weighted ℓ_1 norm has much more sparsity encouraging than the ℓ_1 norm [17]. Meanwhile, based on group sparse representation, we have proven that WNNM, NNM are equivalent to the weighted ℓ_1 norm minimization and ℓ_1 norm minimization, respectively. Therefore, we prove that WNNM is more accurate than NNM. \square

Theorem 5. Defining $X, L \in \Re^N, X_i, L_i \in \Re^{m \times k}$, and e(j) as each element of error vector e, where e = X - L, j = 1, ..., N. Assume that e(j) follows an independent zero mean distribution with variance δ^2 , and thus for any $\varepsilon > 0$, we can represent the relationship between $\frac{1}{N}||X - L||_2^2$ and $\frac{1}{K}\sum_{i=1}^n ||X_i - L_i||_2^2$ by the following property,

$$\lim_{\substack{N \to \infty \\ K \to \infty}} \mathbf{P}\{|\frac{1}{N}||\mathbf{X} - \mathbf{L}||_2^2 - \frac{1}{K} \sum_{i=1}^n ||\mathbf{X}_i - \mathbf{L}_i||_F^2| < \varepsilon\} = 1$$
(46)

where $P(\bullet)$ represents the probability and $K = m \times k \times n$.

Proof. Owing to the assumption that e(j) follows an independent zero mean distribution with variance δ^2 , namely, E[e(j)] = 0 and $Var[e(j)] = \delta^2$. Thus, it can be deduced that each $e(j)^2$ is also independent, and the meaning of each $e(j)^2$ is:

$$E[e(j)^{2}] = Var[e(j)] + [E[e(j)]]^{2} = \delta^{2}, j = 1, 2, ..., N$$
 (47)

By invoking the *law of Large numbers* in probability theory, for any $\varepsilon > 0$, it leads to $\lim_{N \to \infty} P\{|\frac{1}{N} \sum_{j=1}^{N} e(j)^2 - \delta^2| < \frac{\varepsilon}{2}\} = 1$, namely,

$$\lim_{N \to \infty} P\{ \left| \frac{1}{N} ||X - L||_2^2 - \delta^2 \right| < \frac{\varepsilon}{2} \} = 1$$
 (48)

Next, we denote the concatenation of all the groups X_i and L_i , i=1,2,...,n, by X and L, respectively. Meanwhile, we denote the error of each element of X-L by e(k), k=1,2,...,K. We have also denote e(k) following an independent zero mean distribution with variance δ^2 .

Therefore, the same process applied to $e(k)^2$ yields $\lim_{N\to\infty} P\{|\frac{1}{N}\Sigma_{k=1}^N e(k)^2 - \delta^2| < \frac{\varepsilon}{2}\} = 1$, i.e.,

$$\lim_{N \to \infty} \mathbf{P}\{|\frac{1}{N}\sum_{i=1}^{n}||\mathbf{X}_{i} - \mathbf{L}_{i}||_{2}^{2} - \delta^{2}| < \frac{\varepsilon}{2}\} = 1$$
 (49)

Obviously, considering Eqs. (48) and (49) together, we can prove Eq. (46).

8. REFERENCES

- [1] Srebro N, Salakhutdinov R R. Collaborative filtering in a non-uniform world: Learning with the weighted trace norm[C]//Advances in Neural Information Processing Systems. 2010: 2056-2064.
- [2] Cai J F, Cands E J, Shen Z. A singular value thresholding algorithm for matrix completion[J]. SIAM Journal on Optimization, 2010, 20(4): 1956-1982.
- [3] Zheng Y, Liu G, Sugimoto S, et al. Practical low-rank matrix approximation under robust ℓ_1 -norm[C]//Computer Vision and Pattern Recognition (CVPR), 2012 IEEE Conference on. IEEE, 2012: 1410-1417.
- [4] Eriksson A, Van Den Hengel A. Efficient computation of robust low-rank matrix approximations in the presence of missing data using the ℓ_1 -norm[C]//Computer Vision and Pattern Recognition (CVPR), 2010 IEEE Conference on. IEEE, 2010: 771-778.
- [5] Ke Q, Kanade T. Robust ℓ_1 -norm factorization in the presence of outliers and missing data by alternative convex programming[C]//Computer Vision and Pattern Recognition, 2005. CVPR 2005. IEEE Computer Society Conference on. IEEE, 2005, 1: 739-746.

- [6] Fazel M. Matrix rank minimization with applications[D]. PhD thesis, Stanford University, 2002.
- [7] Cands E J, Li X, Ma Y, et al. Robust principal component analysis?[J]. Journal of the ACM (JACM), 2011, 58(3): 11.
- [8] Liu G, Lin Z, Yu Y. Robust subspace segmentation by low-rank representation[C]//Proceedings of the 27th international conference on machine learning (ICML-10). 2010: 663-670.
- [9] Gu S, Zhang L, Zuo W, et al. Weighted nuclear norm minimization with application to image denoising[C]//Proceedings of the IEEE Conference on Computer Vision and Pattern Recognition. 2014: 2862-2869.
- [10] Lu C, Tang J, Yan S, et al. Generalized nonconvex nonsmooth low-rank minimization[C]//Proceedings of the IEEE Conference on Computer Vision and Pattern Recognition. 2014: 4130-4137.
- [11] Sadigh D, Ohlsson H, Sastry S S, et al. Robust subspace system identification via weighted nuclear norm optimization[J]. IFAC Proceedings Volumes, 2014, 47(3): 9510-9515.
- [12] Chen F, Zhang L, Yu H. External patch prior guided internal clustering for image denoising[C]//Proceedings of the IEEE International Conference on Computer Vision. 2015: 603-611.
- [13] Aharon M, Elad M, Bruckstein A. *k*-SVD: An algorithm for designing overcomplete dictionaries for sparse representation[J]. IEEE Transactions on signal processing, 2006, 54(11): 4311-4322.
- [14] Mairal J, Bach F, Ponce J, et al. Non-local sparse models for image restoration[C]//Computer Vision, 2009 IEEE 12th International Conference on. IEEE, 2009: 2272-2279.
- [15] Zhang J, Zhao D, Gao W. Group-based sparse representation for image restoration[J]. IEEE Transactions on Image Processing, 2014, 23(8): 3336-3351.
- [16] Zha Z, Liu X, Huang X, et al. Analyzing the group sparsity based on the rank minimization methods[J]. arXiv preprint arXiv:1611.08983, 2016.
- [17] Candes E J, Wakin M B, Boyd S P. Enhancing sparsity by reweighted ℓ_1 minimization[J]. Journal of Fourier analysis and applications, 2008, 14(5): 877-905.
- [18] Candes E, Recht B. Exact matrix completion via convex optimization[J]. Communications of the ACM, 2012, 55(6): 111-119.

- [19] Li C, Yin W, Zhang Y. Users guide for TVAL3: TV minimization by augmented lagrangian and alternating direction algorithms[J]. CAAM report, 2009, 20: 46-47.
- [20] Beck A, Teboulle M. Fast gradient-based algorithms for constrained total variation image denoising and deblurring problems[J]. IEEE Transactions on Image Processing, 2009, 18(11): 2419-2434.
- [21] Boyd S, Parikh N, Chu E, et al. Distributed optimization and statistical learning via the alternating direction method of multipliers[J]. Foundations and Trends? in Machine Learning, 2011, 3(1): 1-122.
- [22] Chang S G, Yu B, Vetterli M. Adaptive wavelet thresholding for image denoising and compression[J]. IEEE Transactions on image processing, 2000, 9(9): 1532-1546.
- [23] Danielyan A, Katkovnik V, Egiazarian K. BM3D frames and variational image deblurring[J]. IEEE Transactions on Image Processing, 2012, 21(4): 1715-1728.
- [24] Dong W, Zhang L, Shi G, et al. Nonlocally centralized sparse representation for image restoration[J]. IEEE Transactions on Image Processing, 2013, 22(4): 1620-1630.
- [25] Xu Y, Yin W. A fast patch-dictionary method for whole image recovery[J]. arXiv preprint arXiv:1408.3740, 2014.
- [26] Papyan V, Elad M. Multi-scale patch-based image restoration[J]. IEEE Transactions on image processing, 2016, 25(1): 249-261.
- [27] Mun S, Fowler J E. Block compressed sensing of images using directional transforms[C]//Image Processing (ICIP), 2009 16th IEEE International Conference on. IEEE, 2009: 3021-3024.
- [28] Egiazarian K, Foi A, Katkovnik V. Compressed sensing image reconstruction via recursive spatially adaptive filtering[C]//Image Processing, 2007. ICIP 2007. IEEE International Conference on. IEEE, 2007, 1: I-549-I-552.
- [29] Dong W, Shi G, Li X, et al. Image reconstruction with locally adaptive sparsity and nonlocal robust regularization[J]. Signal Processing: Image Communication, 2012, 27(10): 1109-1122.
- [30] Zhang J, Zhao D, Jiang F, et al. Structural group sparse representation for image compressive sensing recovery[C]//Data Compression Conference (DCC), 2013. IEEE, 2013: 331-340.
- [31] Canh T N, Dinh K Q, Jeon B. Multi-scale/multi-resolution Kronecker compressive imaging[C]//Image Processing (ICIP), 2015 IEEE International Conference on. IEEE, 2015: 2700-2704.

- [32] Gu S, Xie Q, Meng D, et al. Weighted nuclear norm minimization and its applications to low level vision[J]. International Journal of Computer Vision, 2016: 1-26.
- [33] Lu C, Tang J, Yan S, et al. Nonconvex nonsmooth low rank minimization via iteratively reweighted nuclear norm[J]. IEEE Transactions on Image Processing, 2016, 25(2): 829-839.
- [34] Lewis A S. The convex analysis of unitarily invariant matrix functions[J]. Journal of Convex Analysis, 1995, 2(1): 173-183.
- [35] Dong W, Shi G, Li X, et al. Compressive sensing via nonlocal low-rank regularization[J]. IEEE Transactions on Image Processing, 2014, 23(8): 3618-3632.